Macrocycles

International Edition: DOI: 10.1002/anie.201809514
German Edition: DOI: 10.1002/ange.201809514

Reversible Photoisomerization of Monolayers of π-Expanded Oligothiophene Macrocycles at Solid–Liquid Interfaces

*José D. Cojal González, Masahiko Iyoda, and Jürgen P. Rabe**

Abstract: *Self-assembled monolayers of a π-expanded oligothiophene macrocycle undergo photoisomerization between their Z,Z and E,E diastereomers at the interface between octanoic acid solutions and highly oriented pyrolytic graphite (HOPG). The switching process proceeds in situ at the solid–liquid interface and was followed by scanning tunneling microscopy (STM). Upon illumination with light at 365 nm (546 nm), a monolayer of Z,Z-8mer (E,E-8mer) photoisomerizes to the E,E-8mer (Z,Z-8mer) form with changes in 2D hexagonal packing. These findings provide insight towards the design of photoresponsive surfaces with desirable optoelectronic and structural (host–guest) properties.*

Macrocyclic oligothiophenes and their π-extended derivatives are regarded as "infinite" π-conjugated systems, with a structurally well-defined oligomer, and free from effects of terminal groups. Similar to their linear counterparts, π-expanded macrocyclic oligothiophenes have attracted attention for their potential applications in molecular electronics[1–3] and as components in molecular devices.[4–6] Moreover, their structural characteristics with shape-persistent inner cavities allow small molecules to be incorporated in the cavities as guests to produce supramolecular structures with unusual chemical and electronic properties.[7–9]

Fully conjugated π-expanded oligothiophene macrocycles are closely related to redox-active oligothiophene macrocycles, which exhibit great potential for optoelectronic applications, organic solar cells, and field-effect transistors, among many others.[10] Tailoring such functional materials at surfaces is therefore highly attractive. Moreover, the design of photoresponsive switchable monolayers is of particular interest towards the development of smart surfaces and interfaces.[11,12] Diarylethene- and azobenzene-containing molecules are among the most common choices to fabricate photoswitchable self-assembled monolayers.[13–19] Not only reversibility, but as well the combination of different functionalities such as large structural changes,[20] electronic transport,[21] and host-guest capability,[22] are highly desirable for future generations of versatile photoresponsive molecules and systems.

Absorption spectra of medium to giant π-expanded oligothiophene macrocycles exhibit a linear relationship between their longest absorption maxima and the reciprocal of the number of thiophenes, which suggests that these systems maintain considerable π–π overlapping.[23] The modified McMurry coupling reaction method to synthesize π-expanded oligothiophene macrocycles has a high diastereomeric selectivity towards production of only *E*,*E* diastereomers for large macrocycles (≥ 9 thiophene units) and *Z*,*Z* diastereomers for small ones (≤ 6 thiophene units).[6] The case of macrocycles with two stable diastereomers *E*,*E* and *Z*,*Z* is therefore unique for eight units of thiophene. We have previously reported on the photoisomerization between *Z*,*Z*-8mer and *E*,*E*-8mer for cyclohexane solutions.[24]

Furthermore, the macrocycle *E*,*E*-8mer can incorporate fullerene C_{60} in its inner cavity to form a Saturn-like complex thanks to the van der Waals interactions between C_{60} and the sulfur atoms of the thiophene units.[24] These complex formation capabilities of *E*,*E*-8mer, together with the photoswitching properties of *E*,*E*-8mer↔*Z*,*Z*-8mer and the adsorption of 8-mers on either HOPG[24] or as complex on templated HOPG,[9] render 8-mers good candidates for versatile photoresponsive materials.

Scanning tunneling microscopy (STM) is a well stablished and versatile technique to investigate physical, chemical, and structural properties of molecules at surfaces.[25–27] STM at the solid–liquid interface[28–30] represents an efficient approach to study in situ dynamic processes involving interfaces, such as photoswitching[13,17–19] and chemical reactions.[31–34]

Herein, we introduce self-assembled monolayers of the diastereomers *Z*,*Z*-8mer and *E*,*E*-8mer at solid–liquid interfaces, which undergo in situ photoisomerization upon irradiation with UV/visible light (Scheme 1).

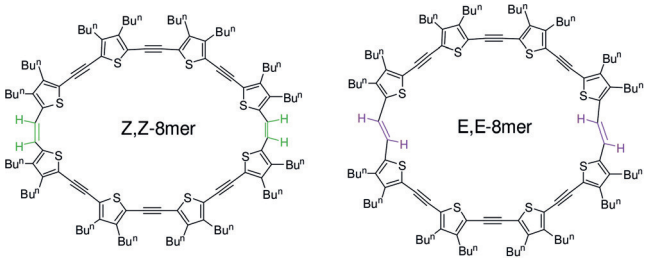

Scheme 1. Chemical structures of *Z*,*Z*-8mer and *E*,*E*-8mer.

[*] Dr. J. D. Cojal González, Prof. Dr. J. P. Rabe
Department of Physics & IRIS Adlershof
Humboldt-Universität zu Berlin
Newtonstr. 15, 12489 Berlin (Germany)
E-mail: rabe@physik.hu-berlin.de
Prof. Dr. M. Iyoda
Department of Chemistry
Graduate School of Science and Engineering
Tokyo Metropolitan University
Hachioji, Tokyo 192-0397 (Japan)
Supporting information and the ORCID identification number(s) for the author(s) of this article can be found under: https://doi.org/10.1002/anie.201809514.

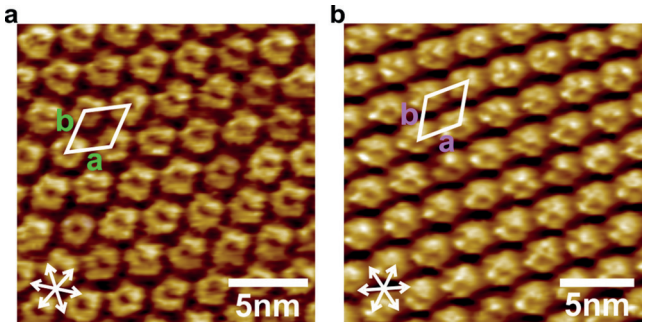

Figure 1. STM height images, unit cell dimensions, and imaging conditions. a) *Z*,*Z*-8mer: $a_{ZZ} = (2.81 \pm 0.04)$ nm, $b_{ZZ} = (2.78 \pm 0.03)$ nm, $\theta_{ZZ} = (61 \pm 1)°$; $U_s = -1.14$ V and $I_t = 95$ pA. b) *E*,*E*-8mer: $a_{EE} = (2.92 \pm 0.03)$ nm, $b_{EE} = (2.89 \pm 0.02)$ nm, $\theta_{EE} = (60.5 \pm 0.6)°$; $U_s = -0.77$ V and $I_t = 100$ pA. The unit cell parameters were determined from at least ten experimental values.

Figure 1 displays STM images of the macrocycles at the interface between their solution in octanoic acid and the basal plane of graphite. The π-electron-conjugated cores are observed as ellipsoidal (*Z*,*Z*-8mer) or circular (*E*,*E*-8mer) high-contrast moieties. Owing to the large difference in the size of the energy gap,[24] the alkyl chains cannot be resolved simultaneously.[35,36] In fact, the n-butyl side chains are unevenly distributed between backfolded upwards, downwards, and in plane.[9]

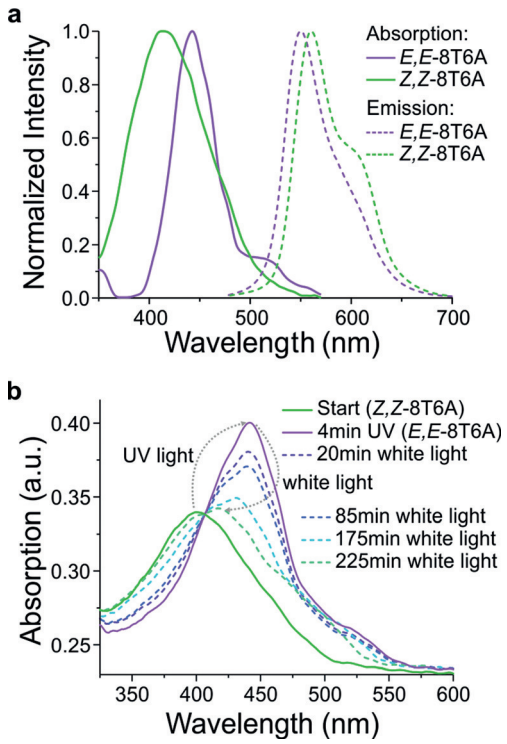

Figure 2. a) Absorption and emission spectra of *E*,*E*-8mer and *Z*,*Z*-8mer in octanoic acid, with excitation at 436 nm. b) Photoisomerization of an octanoic acid solution of *Z*,*Z*-8mer (solid green line), which isomerized to *E*,*E*-8mer (solid purple line) upon irradiation with UV light at 365 nm. Further irradiation using a white fluorescent lamp led to slow isomerization back to *Z*,*Z*-8mer (dashed lines).

Figure 2a shows the significantly different UV/Vis spectra for both diastereomers *E*,*E*-8mer and *Z*,*Z*-8mer in octanoic acid solutions, while the maxima of emission upon excitation at 436 nm are very close in the same solution. Moreover, irradiation of a solution of *Z*,*Z*-8mer in octanoic acid with UV light at 365 nm produces *E*,*E*-8mer after 4 min (Figure 2b). Further irradiation of the latter solution with a white fluorescent lamp leads to slow recovery of the original spectrum of *Z*,*Z*-8mer.

In order to reproduce the switching results at the solid–liquid interface, we employed our home-built STM placed on an optical table equipped with a multimode optical fiber for direct in situ illumination of the sample. An octanoic acid solution of either *Z*,*Z*-8mer or *E*,*E*-8mer with a concentration of 5×10^{-5} M was applied to the basal plane of freshly cleaved HOPG. Several images were recorded at different positions on the sample, and corrected with respect to the hexagonal HOPG lattice underneath. STM images of *Z*,*Z*-8mer before and after illumination at the octanoic acid/graphite interface are shown in Figure 3. The low intensity of the irradiation (UV at ca. 0.8 mW cm^{-2} for 5–30 min) allowed us to follow structural changes while scanning. The increment in the temperature of the solvent due to the irradiation is estimated to be as small as 0.1 K min^{-1} at maximum power, neglecting even possible energy transfer to the substrate.

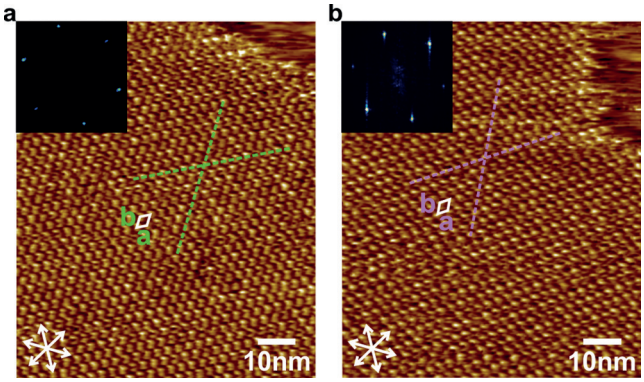

Figure 3. a) STM height image and FFT (inset) recorded before irradiation of a sample of *Z*,*Z*-8mer. Tunneling voltage $U_s = -0.20$ V and tunneling current $I_t = 110$ pA. b) STM height image and FFT of the same region after 11 min of irradiation with UV light. $U_s = -0.30$ V and $I_t = 100$ pA. Dashed lines show the orientation of the unit cell axis of the adsorbed molecules.

The conversion of *Z*,*Z*-8mer into *E*,*E*-8mer upon UV illumination takes place after several minutes and varies from experiment to experiment between 5 and 30 min. Figure 3 depicts structural changes in the 2D arrangement after 11 min of illumination with UV light. Fast Fourier transforms (FFTs) indicate an increase in the average unit cell size (from 6 images before and after illumination) from $a_{ZZ} = (2.82 \pm 0.02)$ nm, $b_{ZZ} = (2.83 \pm 0.02)$ nm, $\theta_{ZZ} = (60 \pm 1)°$ to $a_{EE} = (2.93 \pm 0.03)$ nm, $b_{EE} = (2.94 \pm 0.03)$ nm, $\theta_{EE} = (61 \pm 1)°$. Moreover, the orientation of the adsorbed molecules changes by $(7 \pm 1)°$, as marked with dashed lines in each Figure. The orientation with respect to the underlying graphene changes

consequently from 25° to 32°. A domain boundary at the top right part of each image marks a region with lower stability, which enhances dynamics[29] and is used here as a point of reference.

The transition between the unit cells in Figure 3 happens gradually. First the ordered region in Figure 3a becomes disordered, which can be quantified as the number of non-redundant peaks in the FFT increases as the UV illumination proceeds (see the Supporting Information, Figures S1 and S2). Eventually the double peaks detected in the FFT fade out to the ones corresponding with the new unit cell of *E*,*E*-8mer (Figure 3b).

The reverse switching from a 2D monolayer of *E*,*E*-8mer to the corresponding monolayer of its photoisomer *Z*,*Z*-8mer is achieved upon irradiation with light at 546 ± 16 nm. This conversion typically takes less time than the reverse one. In Figure 4, an image is displayed of a sample of *E*,*E*-8mer that had been irradiated for 2 min (imaging a 100 nm × 100 nm sample size takes around 2 min to complete), where a sudden change in the orientation and size of the ordered monolayer is registered while scanning a single frame. The lower part of Figure 4a corresponds to the initial *E*,*E*-8mer monolayer, which from the FFT (intensities marked in magenta circles) gives a unit cell of $a_{EE} = (2.87 \pm 0.31)$ nm, $b_{EE} = (2.97 \pm 0.31)$ nm, and $\theta_{EE} = (59 \pm 3)°$. The upper part of the STM image corresponds to the intensities marked by the white circles, which gives a unit cell of $a_{ZZ} = (2.79 \pm 0.22)$ nm, $b_{ZZ} = (2.81 \pm 0.22)$ nm, and $\theta_{ZZ} = (59 \pm 2)°$, and is attributed to the *Z*,*Z*-8mer. A change in the orientation by (14 ± 2)° was also measured. The relatively large errors of the unit cell dimensions here are due to the small sample size and the noisy nature of the sampling. Figure 4c shows a typical *E*,*E*-8mer sample before illumination with an average unit cell (from 8 images) of $a_{EE} = (2.90 \pm 0.02)$ nm, $b_{EE} = (2.92 \pm 0.02)$ nm, and $\theta_{EE} = (60 \pm 1)°$. On the other hand, after 12 min of illumination with light at 546 nm, an average unit cell (out of 7 images) of $a_{ZZ} = (2.82 \pm 0.01)$ nm, $b_{ZZ} = (2.82 \pm 0.02)$ nm, and $\theta_{ZZ} = (60.6 \pm 0.7)°$ was determined, corresponding to the unit cell of *Z*,*Z*-8mer.

In solution, the photoisomerization process between *E*,*E*-8mer and *Z*,*Z*-8mer is a two-step reaction, involving first the formation of the transition isomer *E*,*Z*-8mer, which has been detected as a side product of the photochemical reaction.[24] In the present experiment, we deduce that the photoisomerization process happens at the solid–liquid interface with a contribution from the (few) molecules isomerized in the bulk liquid, which are in dynamic equilibrium with those in the molecular assembly.[13,29] Each photochemical transformation between *Z*,*Z*-8mer and *E*,*E*-8mer takes place smoothly.[24] Moreover, almost all molecules in the 5 µL drop (ca. 10^{13}) were adsorbed on the HOPG surface in an area of 1 cm^2. Therefore, almost all molecules forming self-assembled monolayers were photoexcited on the HOPG surface. After the first photoexcitation of *E*,*E*-8mer, for example, a small amount of *E*,*E*-8mer is transformed into *Z*,*Z*-8mer. In the next step, an energy transfer from the excited *E*,*E*-8mer to the non-excited, labilized *E*,*E*-8mer close to be photoisomerized *Z*,*Z*-8mer may occur owing to the

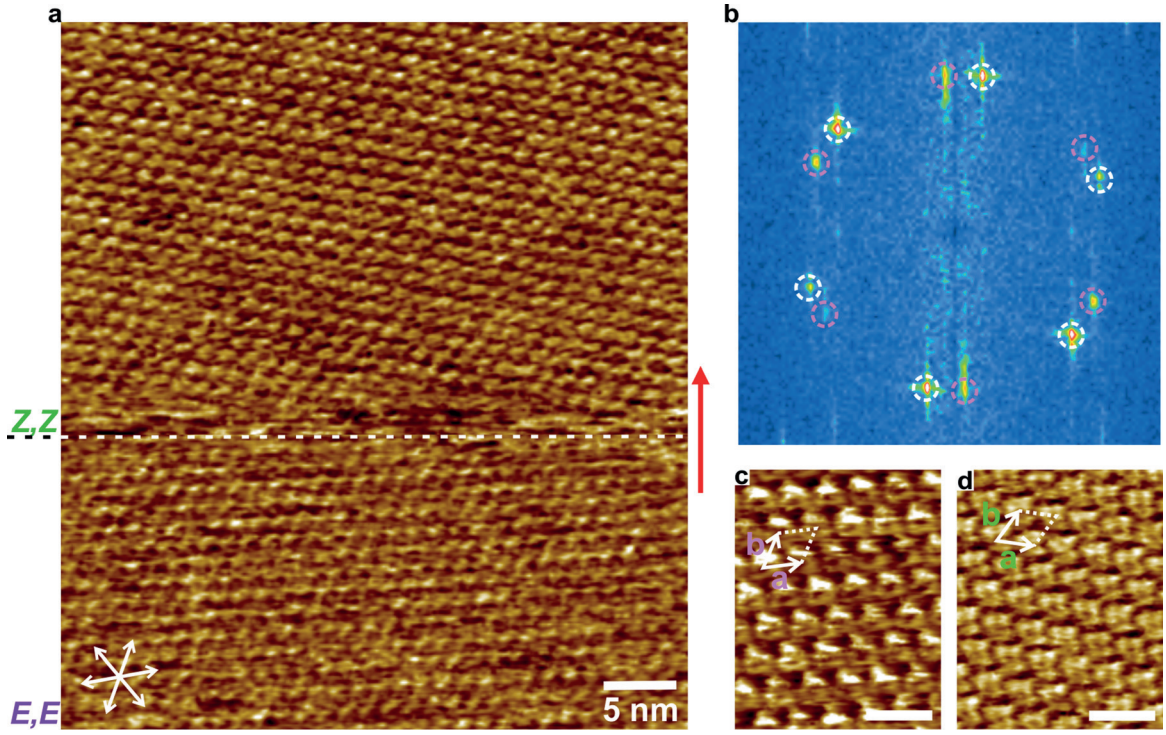

Figure 4. a) STM height image showing the transition between monolayer order for *E*,*E*-8mer (below the white dotted line) to *Z*,*Z*-8mer after irradiation at 546 ± 16 nm. The red arrow indicates the scan direction. Scale bar: 10 nm. b) FFT image showing both hexagonal patterns. The one connecting the magenta circles corresponds to the unit cell of *E*,*E*-8mer while the white circles mark the *Z*,*Z*-8mer one. c) STM height image of *E*,*E*-8mer taken before irradiation. Scale bar: 5 nm. d) STM height image of *Z*,*Z*-8mer recorded 10 min after the transition image in (a). Scale bar: 5 nm. STM conditions for all images: $U_s = -1.23$ V and $I_t = 95$ pA.

lattice strain. Finally, photoisomerized *Z*,*Z*-8mer may occupy the main area on the HOPG surface.

The experiments detailed above were repeated at least four times for different samples, meaning different tips and freshly cleaved HOPG substrates. We were not able to detect precise indications of the transition between unit cells in all attempts, but for all of them, several unit cell parameters could be measured before and after the irradiation. Figure 5 presents the results of these photoconversion experiments. A covariance matrix plot shows the changes in the unit cell

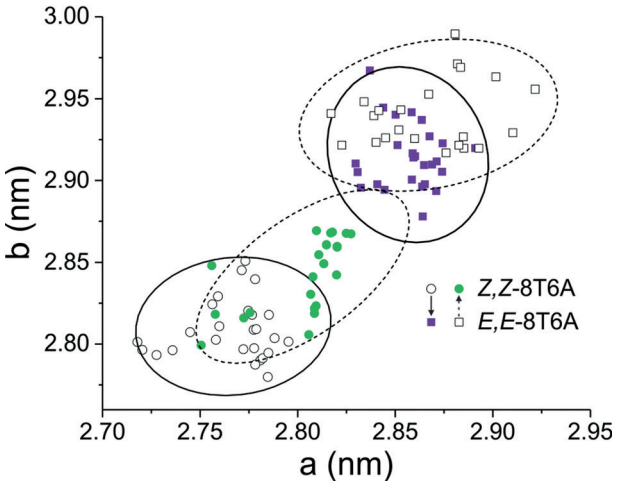

Figure 5. Covariance matrix plot showing the measured unit cells before and after sample irradiation. From *Z*,*Z*-8mer (empty circles) to *E*,*E*-8mer (filled purple squares), the switching occurs after using a UV LED source at 365 nm. From *E*,*E*-8mer (empty squares) to *Z*,*Z*-8mer (filled green circles), the switching occurs with a TRITC filter set (546 nm). Ellipsoids are drawn with a 90% of confidence level.

parameters *a* and *b* starting from *Z*,*Z*-8mer (empty circles) and from *E*,*E*-8mer (empty squares) to the photoisomers *E*,*E*-8mer (filled squares) and *Z*,*Z*-8mer (filled circles) upon irradiation with UV light and green light (546 nm), respectively. Each square or circle represents a unit cell measurement in a different region of the sample.

The average unit cell for all initial *Z*,*Z*-8mer ordered monolayers is $a_{ZZ} = (2.77 \pm 0.04)$ nm, $b_{ZZ} = (2.81 \pm 0.03)$ nm, and $\theta_{ZZ} = (60.8 \pm 0.8)°$, which after switching changes to $a_{EE} = (2.86 \pm 0.03)$ nm, $b_{EE} = (2.91 \pm 0.03)$ nm, and $\theta_{EE} = (60.4 \pm 0.5)°$. On the other hand, starting from monolayers of *E*,*E*-8mer, the average unit cell is $a_{EE} = (2.87 \pm 0.04)$ nm, $b_{EE} = (2.93 \pm 0.03)$ nm, and $\theta_{EE} = (60.3 \pm 0.8)°$, and after switching, it is $a_{ZZ} = (2.80 \pm 0.05)$ nm, $b_{ZZ} = (2.84 \pm 0.04)$ nm, and $\theta_{ZZ} = (60.7 \pm 0.7)°$. The fact that the unit cell parameters for the isomerized *Z*,*Z*-8mer are slightly larger than the ones for the pristine *Z*,*Z*-8mer is indicative of an incomplete reaction and possible contamination of not isomerized *E*,*E*-8mer and incomplete isomerized *E*,*Z*-8mer (transition isomer) molecules in the newly formed *Z*,*Z*-8mer monolayer, which, however, does not affect the order of the array.

We evaluated as well the change in the orientation of the unit cells in the photoisomerization experiments (schematically shown in Figure S3). The detection of regions with coexistence of both crystalline domains is rare as the illumination is not localized but occurs over the whole scanning area. The change in the orientation with respect to the underneath HOPG was determined by averaging the orientation of at least four images before and after the transition was detected (as in Figure 3), and only in one case (Figure 4) both orientations were clearly detected in a single STM image. The average change in orientation for five transitions *E*,*E*-8mer→*Z*,*Z*-8mer and five transitions *Z*,*Z*-8mer→*E*,*E*-8mer was $(10 \pm 4)°$, with an average orientation of $(26 \pm 6)°$ for *Z*,*Z*-8mer and $(36 \pm 6)°$ for *E*,*E*-8mer. Despite the relatively large error, we consistently measured a rotation in the unit cell orientation of the self-assembled monolayers in all experiments, which validates further the photoisomerization reaction upon illumination.

In summary, by using STM we have provided the first evidence for the in situ reversible photoswitching of π-expanded oligothiophenes between the stable forms *E*,*E*- and *Z*,*Z*-8mers at the solid–liquid interface. Short-time irradiation with UV light or green light, respectively, of a highly ordered self-assembly of *Z*,*Z*-8mer or *E*,*E*-8mer led to the formation of a similarly ordered 2D hexagonal network of the other diastereomer. The in situ conversion between unit cells and the change in the orientation of the adsorbed macrocycles showed that the photoisomerization process is kinetically favorable and happens at the solid–liquid interface, with some possible contribution from molecules isomerized in the bulk liquid. To the best of our knowledge and taking into account the host–guest capabilities of these π-expanded macrocycles, these results provide the first example of switchable macrocycles in self-assembled monolayers at solid–liquid interfaces, with capabilities to create photoresponsive cargo delivery systems.

Acknowledgements

This work was funded by the Deutsche Forschungsgemeinschaft (DFG) through SFB 765, SFB 951 (Projektnummer 182087777), and Ra482/6-1, as well as the Strategic International Research Cooperative Program (SICP) [Strategic Japanese-German Cooperation Program from JST].

Conflict of interest

The authors declare no conflict of interest.

Keywords: macrocycles · photoisomerization · photoresponsive surfaces · scanning tunneling microscopy · self-assembly

How to cite: *Angew. Chem. Int. Ed.* **2018**, *57*, 17038–17042
Angew. Chem. **2018**, *130*, 17284–17288

[1] J. M. Tour, *Acc. Chem. Res.* **2000**, *33*, 791–804.
[2] D. Fichou, *J. Mater. Chem.* **2000**, *10*, 571–588.
[3] T. Otsubo, Y. Aso, K. Takimiya, *J. Mater. Chem.* **2002**, *12*, 2565–2575.
[4] J. Krömer, I. Rios-Carreras, G. Fuhrmann, C. Musch, M. Wunderlin, T. Debaerdemaeker, E. Mena-Osteritz, P. Bäuerle,

Angew. Chem. Int. Ed. **2000**, *39*, 3481 – 3486; *Angew. Chem.* **2000**, *112*, 3623 – 3628.
[5] M. Mayor, C. Didschies, *Angew. Chem. Int. Ed.* **2003**, *42*, 3176 – 3179; *Angew. Chem.* **2003**, *115*, 3284 – 3287.
[6] M. Iyoda, H. Shimizu, *Chem. Soc. Rev.* **2015**, *44*, 6411 – 6424.
[7] E. Mena-Osteritz, P. Bäuerle, *Adv. Mater.* **2006**, *18*, 447 – 451.
[8] G.-B. Pan, X.-H. Cheng, S. Höger, W. Freyland, *J. Am. Chem. Soc.* **2006**, *128*, 4218 – 4219.
[9] J. D. Cojal González, M. Iyoda, J. P. Rabe, *Nat. Commun.* **2017**, *8*, 14717.
[10] A. Mishra, C.-Q. Ma, J. L. Segura, P. Bäuerle in *Handbook of Thiophene-Based Materials* (Eds.: I. F. Perepichka, D. F. Perepichka), Wiley, Hoboken, **2009**, pp. 1 – 155.
[11] D. Wang, Q. Chen, L.-J. Wan, *Phys. Chem. Chem. Phys.* **2008**, *10*, 6467 – 6478.
[12] W. R. Browne, B. L. Feringa, *Annu. Rev. Phys. Chem.* **2009**, *60*, 407 – 428.
[13] C. L. Feng, Y. Zhang, J. Jin, Y. Song, L. Xie, G. Qu, L. Jiang, D. Zhu, *Surf. Sci.* **2002**, *513*, 111 – 118.
[14] S. J. van der Molen, H. van der Vegte, T. Kudernac, I. Amin, B. L. Feringa, B. J. van Wees, *Nanotechnology* **2006**, *17*, 310.
[15] N. Katsonis, T. Kudernac, M. Walko, S. J. van der Molen, B. J. van Wees, B. L. Feringa, *Adv. Mater.* **2006**, *18*, 1397 – 1400.
[16] M. Alemani, M. V. Peters, S. Hecht, K.-H. Rieder, F. Moresco, L. Grill, *J. Am. Chem. Soc.* **2006**, *128*, 14446 – 14447.
[17] D. Bléger, A. Ciesielski, P. Samorí, S. Hecht, *Chem. Eur. J.* **2010**, *16*, 14256 – 14260.
[18] S. Bonacchi, M. El Garah, A. Ciesielski, M. Herder, S. Conti, M. Cecchini, S. Hecht, P. Samorì, *Angew. Chem. Int. Ed.* **2015**, *54*, 4865 – 4869; *Angew. Chem.* **2015**, *127*, 4947 – 4951.
[19] M. E. Garah, E. Borré, A. Ciesielski, A. Dianat, R. Gutierrez, G. Cuniberti, S. Bellemin-Laponnaz, M. Mauro, P. Samorì, *Small* **2017**, https://doi.org/10.1002/smll.201701790.
[20] C. Weber, T. Liebig, M. Gensler, A. Zykov, L. Pithan, J. P. Rabe, S. Hecht, D. Bléger, S. Kowarik, *Sci. Rep.* **2016**, *6*, 25605.
[21] Z. J. Donhauser et al., *Science* **2001**, *292*, 2303 – 2307.
[22] Y.-W. Yang, Y.-L. Sun, N. Song, *Acc. Chem. Res.* **2014**, *47*, 1950 – 1960.
[23] K. Nakao, M. Nishimura, T. Tamachi, Y. Kuwatani, H. Miyasaka, T. Nishinaga, M. Iyoda, *J. Am. Chem. Soc.* **2006**, *128*, 16740 – 16747.
[24] H. Shimizu, J. D. Cojal González, M. Hasegawa, T. Nishinaga, T. Haque, M. Takase, H. Otani, J. P. Rabe, M. Iyoda, *J. Am. Chem. Soc.* **2015**, *137*, 3877 – 3885.
[25] J. P. Rabe, *Angew. Chem. Int. Ed. Engl.* **1989**, *28*, 117 – 122; *Angew. Chem.* **1989**, *101*, 117 – 122.
[26] S. De Feyter, F. C. De Schryver, *Chem. Soc. Rev.* **2003**, *32*, 139 – 150.
[27] J. V. Barth, G. Costantini, K. Kern, *Nature* **2005**, *437*, 671 – 679.
[28] J. P. Rabe, S. Buchholz, *Science* **1991**, *253*, 424 – 427.
[29] S. De Feyter, A. Gesquière, M. M. Abdel-Mottaleb, P. C. M. Grim, F. C. De Schryver, C. Meiners, M. Sieffert, S. Valiyaveettil, K. Müllen, *Acc. Chem. Res.* **2000**, *33*, 520 – 531.
[30] A. Ciesielski, C.-A. Palma, M. Bonini, P. Samorì, *Adv. Mater.* **2010**, *22*, 3506 – 3520.
[31] R. Heinz, A. Stabel, J. P. Rabe, G. Wegner, F. C. De Schryver, D. Corens, W. Dehaen, C. Süling, *Angew. Chem. Int. Ed. Engl.* **1994**, *33*, 2080 – 2083; *Angew. Chem.* **1994**, *106*, 2154 – 2157.
[32] J. F. Dienstmaier, D. D. Medina, M. Dogru, P. Knochel, T. Bein, W. M. Heckl, M. Lackinger, *ACS Nano* **2012**, *6*, 7234 – 7242.
[33] D. den Boer, M. Li, T. Habets, P. Iavicoli, A. E. Rowan, R. J. M. Nolte, S. Speller, D. B. Amabilino, S. De Feyter, J. A. A. W. Elemans, *Nat. Chem.* **2013**, *5*, 621 – 627.
[34] A. Ciesielski, M. E. Garah, S. Haar, P. Kovaříček, J.-M. Lehn, P. Samorì, *Nat. Chem.* **2014**, *6*, 1017.
[35] R. Lazzaroni, A. Calderone, J. L. Brédas, J. P. Rabe, *J. Chem. Phys.* **1997**, *107*, 99 – 105.
[36] M. Iyoda et al., *J. Am. Chem. Soc.* **2014**, *136*, 2389 – 2396.

Manuscript received: August 20, 2018
Revised manuscript received: October 11, 2018
Accepted manuscript online: October 31, 2018
Version of record online: November 30, 2018

